

Gauss-Bonnet Black Holes and Heavy Fermion Metals

R. B. Mann

*Department of Physics, University of Waterloo, 200 University Avenue West,
Waterloo, Ontario, Canada, N2L 3G1*

E-Mail: rbmann@sciborg.uwaterloo.ca

R. Pourhasan

*Department of Physics, University of Waterloo, 200 University Avenue West,
Waterloo, Ontario, Canada, N2L 3G1*

E-Mail: r2pourha@uwaterloo.ca

ABSTRACT: We consider charged black holes in Einstein-Gauss-Bonnet Gravity with Lifshitz boundary conditions. We find that this class of models can reproduce the anomalous specific heat of condensed matter systems exhibiting non-Fermi-liquid behaviour at low temperatures. We find that the temperature dependence of the Sommerfeld ratio is sensitive to the choice of Gauss-Bonnet coupling parameter for a given value of the Lifshitz scaling parameter. We propose that this class of models is dual to a class of models of non-Fermi-liquid systems proposed by Castro-Neto et.al.

Contents

1. Introduction	1
2. Field Equations in $(n + 1)$-dimensions	4
3. Series Solutions	5
3.1 Solutions at large r	5
3.2 Near horizon expansion	7
4. Numerical analysis and Thermodynamic Behaviour	8
4.1 Thermal behaviour	8
4.2 Specific heat and Fermi liquid behaviour	12
5. Closing remarks	14

1. Introduction

The AdS/CFT correspondence conjecture [1] has motivated the development of dual gravity models to describe strongly correlated systems in condensed matter physics (CMT) [2, 3, 4, 5]. This “AdS/CMT” correspondence, while more speculative than its AdS/CFT predecessor, has yielded some tantalizing insights into the behaviour of these systems. Systems of heavy fermions [6] – in which electrons near the Fermi surface of certain materials have an effective mass much larger than the free electron mass – are of particular interest since their behaviour is not that of a conventional Fermi liquid. The ratio of the specific heat to temperature (the Sommerfeld ratio denoted by γ_0), for low temperature, does not become constant but instead rises as the temperature decreases [7]. Indeed, there are some observations confirming that this ratio has logarithmic temperature dependence [8]. On the other hand, Castro Neto et al. proposed a model which predicts that the physical properties of the f-electron compounds at low temperatures are characterized by weak power law behavior, $\gamma_0 \equiv C/T \propto T^{-1+\lambda}$ where $\lambda < 1$ is some characteristic parameter [9, 10]. This has been observed experimentally in a number of non-Fermi liquid materials [11, 12]. Though a full understanding of quantum criticality remains an outstanding problem, it is believed that such non Fermi liquid behaviour is due to the existence of a quantum critical point [13].

Near a critical point many condensed matter systems are described by field theories with anisotropic scaling symmetry of the form

$$t \rightarrow \lambda^z t, \quad \mathbf{x} \rightarrow \lambda \mathbf{x}, \quad (1.1)$$

where $z(\geq 1)$ is a dynamical critical exponent represents the degree of anisotropy between space and time; manifestly $z = 1$ pertains to relativistic systems. Applying the AdS/CMT conjecture entails consideration of spacetimes whose metrics have the asymptotic form

$$ds^2 = \ell^2 \left(-r^{2z} dt^2 + \frac{dr^2}{r^2} + r^2 d\mathbf{x}^2 \right) \quad (1.2)$$

where the coordinates (t, r, x^i) are dimensionless and the only length scale in the geometry is ℓ . Such spacetimes are conjectured to be the gravitational duals to field theories with the scaling properties given in (1.1) [14]. It is straightforward to show that metric (1.2) has the scaling properties in (1.1) provided $r \rightarrow \lambda^{-1} r$ as well.

Recently it was shown that these gravitational duals yield non Fermi liquid behavior for the specific heat of quantum critical system that is qualitatively similar to what is seen in experiments on heavy fermion systems [15]. The effects of finite temperature are induced by the presence of a black hole with the asymptotic form (1.2), and the addition of electromagnetic charge introduces another energy scale that can lead to interesting dynamics. The specific heat was found to scale as $T^{3/2}$ at high temperatures T , whereas at low T the behaviour of the specific heat was sensitive to the scaling exponent z . For $z = 1$ conventional Fermi liquid behaviour was recovered (with the Sommerfeld ratio becoming constant), whereas for $z > 1$ the Sommerfeld ratio increased with T as is observed for several heavy fermion systems.

We consider in this paper the effects of adding in higher-order curvature corrections in the form of a Gauss-Bonnet term on Fermi liquid behaviour. In the context of AdS/CFT correspondence, inclusion of higher powers of the curvature is necessary in order to understand CFTs with different values for their central charges. In the context of condensed matter holography, they modify a number of important quantities, including viscosity, DC conductivity, the superconducting phase transition, and more [16, 17, 18, 19]. The simplest and most natural such term to include in the action is the Gauss-Bonnet term. Gauss-Bonnet gravity is a particular case of Lovelock gravity, which in $(n + 1)$ dimensions yields p -order curvature terms (with $p \leq [n/2]$) in field equations with not more than 2 derivatives of any metric function; terms for which $p > [n/2]$ are total derivatives in the action and so do not contribute to the field equations. To obtain a (3+1)-dimensional CMT, for which a (4+1) dimensional gravity theory is the conjectured dual, it is therefore natural to include a Gauss-Bonnet term on the gravity side since for $n = 4$ we can only have $p \leq 2$.

While we will ultimately be concerned with (3+1)-dimensional CMTs, we shall

formulate our considerations in $(n + 1)$ dimensions, making use of the action

$$I = \int d^{n+1}x \sqrt{-g} \left(R - 2\Lambda + \hat{\alpha} \mathcal{L}_{\text{GB}} - \frac{1}{4} F_{\mu\nu} F^{\mu\nu} - \frac{1}{4} H_{\mu\nu} H^{\mu\nu} - \frac{C}{2} B_\mu B^\mu \right), \quad (1.3)$$

where Λ is the cosmological constant and $\mathcal{L}_{\text{GB}} = R_{\mu\nu\gamma\delta} R^{\mu\nu\gamma\delta} - 4R_{\mu\nu} R^{\mu\nu} + R^2$ is the second order Lovelock (Gauss-Bonnet) Lagrangian. The coefficient $\hat{\alpha}$ has the dimension of $(\text{length})^2$ and can be positive or negative, $F_{\mu\nu} = \partial_{[\mu} A_{\nu]}$ with A_μ the Maxwell gauge field, and $H_{\mu\nu} = \partial_{[\mu} B_{\nu]}$ is the field strength of the Proca field B_μ with mass $m^2 = C$.

Neutral black hole solutions with $\alpha = 0$ have been obtained both analytically and numerically [20, 21, 22]. The $\alpha = 0$ charged case in $(n + 1)$ dimensions has been more recently considered [15, 23, 24]. In addition to obtaining a holographic description of a strongly coupled quantum critical point in 5 dimensions with asymmetric scaling that exhibits the aforementioned anomalous specific heat behaviour at low temperature for heavy fermion metals [23], a more general study [24] of the $\hat{\alpha} = 0$ version of (1.3) found a broad range of charged black hole solutions and a general thermodynamic relationship between energy, entropy, and chemical potential. Solutions to neutral Lovelock-Lifshitz black holes were also recently obtained [25] and their thermodynamic behaviour for spatially flat cases was found to be the same [26] as the $p = 1$ Einsteinian case [22]. Perturbative corrections to the charged Lifshitz case due to a Gauss-Bonnet term ($\alpha \neq 0$) have been computed [28], but full black hole solutions and their implications have not been studied.

We begin by introducing $(n + 1)$ -dimensional equations of motion in sec. (2), where we find the constraints that must be imposed on the constants in (1.3) in order that the asymptotic form (1.2) hold. We then investigate solutions at large r in sec. (3.1), which provide us with useful information about possible solutions due to different choices of α . Near horizon expansions are computed in sec. (3.2), and these are used to assist the numerical methods we employ to find solutions. We analyze the thermodynamic behaviour of these charged Gauss-Bonnet black holes numerically in sec. (4) where we specifically focus on $z = 2$ charged black holes in $(4 + 1)$ dimensions. We find that the Gauss-Bonnet coefficient α plays a role dual to that of the characteristic parameter λ in the Castro Neto et al. model [9, 10]. In fact, if the coefficient α is smaller than a certain minimal value α_m , non-Fermi liquid behaviour is enhanced, and the temperature dependence of the Sommerfeld ratio γ_0 at low temperature can be characterized as a weak power law. However as α increases above α_m the power law dependence of this ratio on the temperature becomes vanishingly small, similar to the $\lambda \rightarrow 1$ limit in the Castro Neto et al. model, which as they claim can be fit with the logarithmic behaviour observed in some non fermi liquid compounds. The Gauss-Bonnet term restores Fermi liquid behaviour for $\alpha \gg \alpha_m$. We propose that Lifshitz-GB charged black holes are gravitational duals to the Castro Neto et al. model. Further numerical calculation reveals that the same

qualitative behaviour happens for arbitrary $z > 1$. We finish our paper by giving some closing remarks pertinent to our results.

2. Field Equations in $(n + 1)$ -dimensions

Using the variational principal the field equations that follow from the action (1.3) are:

$$G_{\mu\nu} + \hat{\alpha} G_{\mu\nu}^{\text{GB}} + \Lambda g_{\mu\nu} = T_{\mu\nu}, \quad (2.1)$$

$$\nabla^\mu H_{\mu\nu} = C B_\nu, \quad (2.2)$$

$$\partial_{[\mu} B_{\nu]} = H_{\mu\nu}, \quad (2.3)$$

$$\nabla^\mu F_{\mu\nu} = 0, \quad (2.4)$$

where

$$T_{\mu\nu} = -\frac{1}{2} \left(\frac{1}{4} F_{\rho\sigma} F^{\rho\sigma} g_{\mu\nu} - F^\rho{}_\mu F_{\rho\nu} + \frac{1}{4} H_{\rho\sigma} H^{\rho\sigma} g_{\mu\nu} - H^\rho{}_\mu H_{\rho\nu} + C \left[\frac{1}{2} B_\rho B^\rho g_{\mu\nu} - B_\mu B_\nu \right] \right) \quad (2.5)$$

is the energy-momentum tensor of gauge fields, $G_{\mu\nu}$ is the Einstein tensor, and $G_{\mu\nu}^{\text{GB}}$ is given as:

$$G_{\mu\nu}^{\text{GB}} = 2(-R_{\mu\sigma\kappa\tau} R^{\kappa\tau\sigma}{}_\nu - 2R_{\mu\rho\nu\sigma} R^{\rho\sigma} - 2R_{\mu\sigma} R^\sigma{}_\nu + R R_{\mu\nu}) - \frac{1}{2} \mathcal{L}_{\text{GB}} g_{\mu\nu}, \quad (2.6)$$

The $(n + 1)$ -dimensional metric that preserves the basic symmetries under consideration can be written as

$$ds^2 = \ell^2 \left(-r^{2z} f^2(r) dt^2 + \frac{g^2(r) dr^2}{r^2} + r^2 d\mathbf{x}^2 \right) \quad (2.7)$$

which is that of a black brane or (if appropriate identifications are carried out) a toroidal black hole.

The gauge fields are assumed to be

$$A_t = \ell r^z \kappa(r), \quad B_t = q \ell r^z f(r) j(r), \quad H_{tr} = q \ell z r^{z-1} g(r) h(r) f(r), \quad (2.8)$$

with all other components either vanishing or being given by antisymmetrization. In order to get Lifshitz geometry (1.2) as the asymptotic form of the metric (2.7), one should demand $f(r) = g(r) = h(r) = j(r) = 1$ and $k(r) = 0$ as r goes to infinity which impose the following constraints over the constants:

$$C = \frac{(n-1)z}{\ell^2}, \quad q^2 = \frac{2(z-1)L^2}{z\ell^2}, \quad \Lambda_{\text{eff}} = -\frac{[(z-1)^2 + n(z-2) + n^2] L^2 + n(n-1)\alpha}{2\ell^4}, \quad (2.9)$$

with the following redefinition

$$L^2 = \ell^2 - 2\alpha, \quad \alpha = (n-2)(n-3)\hat{\alpha} \quad (2.10)$$

where according to eq. (2.9) L^2 should be positive which implies $\alpha < \ell^2/2$ and consequently the cosmological constant Λ_{eff} is always negative. Note that upon setting $z = 1$ in (2.9) we recover an effective cosmological constant dependent on the coupling α rather than the usual AdS cosmological constant, i.e. $\Lambda = -n(n-1)/2\ell^2$.

Applying the ansatz (2.7) to the equation (2.4) yields the solution

$$(r^z \kappa)' = \frac{Q}{r^{n-z}} f g \quad (2.11)$$

where Q is an integration constant related to the Maxwell charge and we have chosen boundary conditions such that the Maxwell vector potential vanishes at the horizon.

Substituting (2.9) and (2.11) into eqs. (2.1-2.3), the field equations reduce to the following system of first order differential equations:

$$r \frac{df}{dr} = \frac{f}{4(n-1)(\ell^2 g^2 - 2\alpha)} \{ 2[(n-1)(z-1)j^2 - z(z-1)h^2 + (z-1)^2 + n(z-2) + n^2] g^4 L^2 + 2\alpha(n-1)(ng^4 + n + 4z - 4) - 2(n-1)(n+2z-2)\ell^2 g^2 - Q^2 r^{2-2n} g^4 \}, \quad (2.12)$$

$$r \frac{dg}{dr} = \frac{g}{4(n-1)(\ell^2 g^2 - 2\alpha)} \{ 2[(n-1)(z-1)j^2 + z(z-1)h^2 - (z-1)^2 - n(z-2) - n^2] g^4 L^2 - 2\alpha n(n-1)(1 + g^4) + 2n(n-1)\ell^2 g^2 + Q^2 r^{2-2n} g^4 \}, \quad (2.13)$$

$$r \frac{dj}{dr} = -\frac{j}{4(n-1)(\ell^2 g^2 - 2\alpha)} \{ 2[(n-1)(z-1)j^2 - z(z-1)h^2 + (z-1)^2 + n(z-2) + n^2] g^4 L^2 + 2\alpha(n-1)(ng^4 + n - 4) - 2(n-1)(n-2)\ell^2 g^2 - Q^2 r^{2-2n} g^4 \} + zgh, \quad (2.14)$$

$$r \frac{dh}{dr} = (n-1)(jg - h). \quad (2.15)$$

3. Series Solutions

3.1 Solutions at large r

Since we wish to understand the effects of the Gauss-Bonnet term on the previously considered [24] $(n+1)$ -dimensional charged Einstein solutions with arbitrary z , we begin by linearizing the system in $(n+1)$ -dimensions. Requiring the general metric (2.7) to asymptotically approach the Lifshitz one, we write

$$\begin{aligned} f(r) &= 1 + wf_1(r), \\ g(r) &= 1 + wg_1(r), \\ j(r) &= 1 + wj_1(r), \\ h(r) &= 1 + wh_1(r) \end{aligned} \quad (3.1)$$

where we note that it is also necessary [20, 21] for $j(r)$ and $h(r)$ to approach unity in order to obtain (1.2).

In previous section, we already introduced equations of motion which are shown in (2.12-2.15). Since $f(r)$ does not contribute to the equations for $g(r)$, $h(r)$ and $j(r)$ let's first study a set involving $\{g, h, j\}$; If one inserts perturbative expansion (3.1) into equations (2.13-2.15) one obtains the equations for small perturbations as

$$r \frac{d}{dr} \begin{pmatrix} g_1 \\ h_1 \\ j_1 \end{pmatrix} = \begin{pmatrix} n & -z(z-1)/(n-1) & 1-z \\ 1-n & n-1 & 1-n \\ M_{31}(n, z, \alpha) & -z(n+z-2)/(n-1) & 2z-1 \end{pmatrix} \begin{pmatrix} g_1 \\ h_1 \\ j_1 \end{pmatrix} + \frac{Q^2}{4(n-1)r^{2n-2}} \begin{pmatrix} 1 \\ 0 \\ 1 \end{pmatrix} \quad (3.2)$$

which is identical to the Einsteinian case except for the term

$$M_{31} \equiv \frac{(n+z-2)\ell^2 - 2(n+3z-4)\alpha}{L^2} \quad (3.3)$$

where we have rescaled $r \rightarrow r/\ell$. We have also included the Maxwell gauge field as a first order perturbation, which means that we substitute $Q^2/r^{2(n-1)} = wQ^2/r^{2(n-1)}$, since its falloff may be slower than other terms in the metric functions.

Solving the set (3.2) one obtains:

$$g_1(r) = -\frac{C_1 G_1}{r^{z+n-1}} - \frac{C_2 G_2}{r^{(z+n-1+\sqrt{\gamma})/2}} - \frac{C_3 G_3}{r^{(z+n-1-\sqrt{\gamma})/2}} - \frac{(n-2z)\ell^2 Q^2}{4\Delta(n-z-1)r^{2n-2}}, \quad (3.4)$$

$$h_1(r) = -\frac{C_1}{r^{z+n-1}} - \frac{C_2}{r^{(z+n-1+\sqrt{\gamma})/2}} - \frac{C_3}{r^{(z+n-1-\sqrt{\gamma})/2}} + \frac{[(2n-z-2)\ell^2 - 2(2n-3)\alpha]\ell^2 Q^2}{4L^2\Delta(n-z-1)r^{2n-2}}, \quad (3.5)$$

$$j_1(r) = -\frac{C_1 J_1}{r^{z+n-1}} - \frac{C_2 J_2}{r^{(z+n-1+\sqrt{\gamma})/2}} - \frac{C_3 J_3}{r^{(z+n-1-\sqrt{\gamma})/2}} - \frac{[(n+z-2)\ell^2 - 2(n+2z-3)\alpha]\ell^2 Q^2}{4L^2\Delta(n-z-1)r^{2n-2}}, \quad (3.6)$$

where

$$\gamma = \frac{((n-3z)^2 + 6n - 2z - 7)\ell^2 - 2(n^2 - 6nz + 6n + 14z + z^2 - 15)\alpha}{L^2}, \quad (3.7)$$

$$\Delta = (n+z-2)(n-z-1)\ell^2 - 2(n^2 - 3n - z + 3)\alpha \quad (3.8)$$

$$G_1 = \frac{z(z-1)L^2}{(n-1)^2\ell^2 - 2(n-1)(n+z-2)\alpha}, \quad G_2 = \frac{z-1}{n-1}, \quad G_3 = \frac{z-1}{n-1}, \quad (3.9)$$

$$J_1 = -\frac{z(n+z-2)\ell^2 - 2(n+2z-3)\alpha}{(n-1)^2\ell^2 - 2(n-1)(n-z+2)\alpha}, \quad (3.10)$$

$$J_2 = \frac{n-3z+1-\sqrt{\gamma}}{2(n-1)}, \quad J_3 = \frac{n-3z+1+\sqrt{\gamma}}{2(n-1)}. \quad (3.11)$$

Substituting above expressions into the equation for small perturbations of $f(r)$

$$\begin{aligned} r \frac{d}{dr} f_1(r) &= \frac{(n-2+2z)\ell^2 - 2(n+4z-4)\alpha}{L^2} g_1(r) - \frac{z(z-1)}{n-1} h_1(r) \\ &+ (z-1)j_1(r) - \frac{\ell^2 Q^2}{4L^2(n-1)r^{2n-2}} \end{aligned} \quad (3.12)$$

we obtain

$$\begin{aligned} f_1(r) &= -\frac{C_1 F_1}{r^{z+n-1}} - \frac{C_2 F_2}{r^{(z+n-1+\sqrt{\gamma})/2}} - \frac{C_3 F_3}{r^{(z+n-1-\sqrt{\gamma})/2}} \\ &+ \frac{[(n+z-2)\ell^2 - 2(n+2z-3)\alpha]\ell^2 Q^2}{4L^2 \Delta(n-1)r^{2n-2}}, \end{aligned} \quad (3.13)$$

with

$$\begin{aligned} F_1 &= \frac{(n+2z-2)\ell^2 - 2(n+4z-4)\alpha}{(n+z-1)L^2} G_1 + \frac{z-1}{n+z-1} J_1 \\ &- \frac{z(z-1)}{(n-1)(n+z-1)}, \end{aligned} \quad (3.14)$$

$$\begin{aligned} F_2 &= \frac{(n+2z-2)\ell^2 - 2(n+4z-4)\alpha}{(n+z-1+\sqrt{\gamma})L^2} G_2 + \frac{2(z-1)}{n+z-1+\sqrt{\gamma}} J_2 \\ &- \frac{2z(z-1)}{(n-1)(n+z-1+\sqrt{\gamma})}, \end{aligned} \quad (3.15)$$

$$\begin{aligned} F_3 &= \frac{(n+2z-2)\ell^2 - 2(n+4z-4)\alpha}{(n+z-1-\sqrt{\gamma})L^2} G_3 + \frac{2(z-1)}{n+z-1-\sqrt{\gamma}} J_3 \\ &- \frac{2z(z-1)}{(n-1)(n+z-1-\sqrt{\gamma})}. \end{aligned} \quad (3.16)$$

There are three eigenmodes, of which two are decaying. The third one might be decaying, growing or independent of r depending on the value of α . There is a zero mode if

$$\alpha^{(0)} = \frac{(n-z-1)\ell^2}{2(n-2)}. \quad (3.17)$$

Accordingly, for $\alpha \geq \alpha^{(0)}$ in order to approach the Lifshitz fixed point asymptotically, fine-tuning of initial values is required when numerically solving the non-linear field equations. However if $\alpha < \alpha^{(0)}$, all three eigenmodes are decaying, yielding a family of solutions with the same event horizon that asymptotically approach the Lifshitz background with different fall-off rates.

3.2 Near horizon expansion

To investigate the near horizon behavior of the solutions we consider the following expansions

$$f(r) = f_0 \sqrt{r-r_0} (1 + f_1(r-r_0) + f_2(r-r_0)^2 + \dots),$$

$$\begin{aligned}
g(r) &= \frac{g_0}{\sqrt{r-r_0}}(1 + g_1(r-r_0) + g_2(r-r_0)^2 + \dots), \\
j(r) &= j_0\sqrt{r-r_0}(1 + j_1(r-r_0) + j_2(r-r_0)^2 + \dots), \\
h(r) &= h_0(1 + h_1(r-r_0) + h_2(r-r_0)^2 + \dots),
\end{aligned} \tag{3.18}$$

where r_0 is assumed to be the horizon radius. Inserting this into Eqs. (2.12-2.15) and demanding the coefficients for each power of $(r-r_0)$ vanish yields relations between the various constant coefficients in terms of r_0 and h_0 . For example g_0 is given by:

$$g_0 = \ell r_0^{1/2} \sqrt{\frac{2(n-1)}{\ell^2 r_0^{2-2n}(Q_{\text{ext}}^2 - Q^2) - 2z(z-1)L^2 h_0^2}} \tag{3.19}$$

where

$$Q_{\text{ext}}^2 \equiv \frac{2}{\ell^2 r_0^{2-2n}} [(n^2 + (z-2)n + (z-1)^2) \ell^2 - (n^2 + (2z-3)n + 2(z-1)^2) \alpha^2] \tag{3.20}$$

is the upper bound for the Maxwell charge for a given α . Since $\alpha < \ell^2/2$ the right hand side of eq. (3.20) is always positive. Clearly Q_{ext} decreases as α increases. Furthermore, from (3.19) we see that real series solutions exist provided

$$h_0 < \sqrt{\frac{\ell^2 r_0^{2-2n}(Q_{\text{ext}}^2 - Q^2)}{2z(z-1)L^2}} \tag{3.21}$$

with $Q \leq Q_{\text{ext}}$. All other constants in the series solutions (3.18) can be obtained in terms of r_0 and h_0 as well but we don't write them here because they are too lengthy.

4. Numerical analysis and Thermodynamic Behaviour

To find numerical solutions for the system of ODE's (2.12-2.15) we apply the shooting method, adjusting initial values for the fields $f(r)$, $g(r)$, $j(r)$ and $h(r)$ and requiring each to approach their asymptotic values of unity. To find these initial values we use the near horizon expansions (3.18) by substituting $r_0 + \varepsilon$ for r where $\varepsilon \ll 1$ and choose some values for r_0 and h_0 such that the fields approach unity at large r to within a certain tolerance of 10^{-8} . While we can obtain explicit numerical solutions for the metric functions, we are interested here in their thermodynamic behaviour, particularly insofar as how the Gauss-Bonnet term modifies the Sommerfeld relation. Throughout we restrict our numerical analysis to 5 dimensions.

4.1 Thermal behaviour

The Hawking temperature of a general black brane (2.7) is

$$T = \frac{r_0^z}{4\pi} \tau_z(r_0, Q, \alpha), \tag{4.1}$$

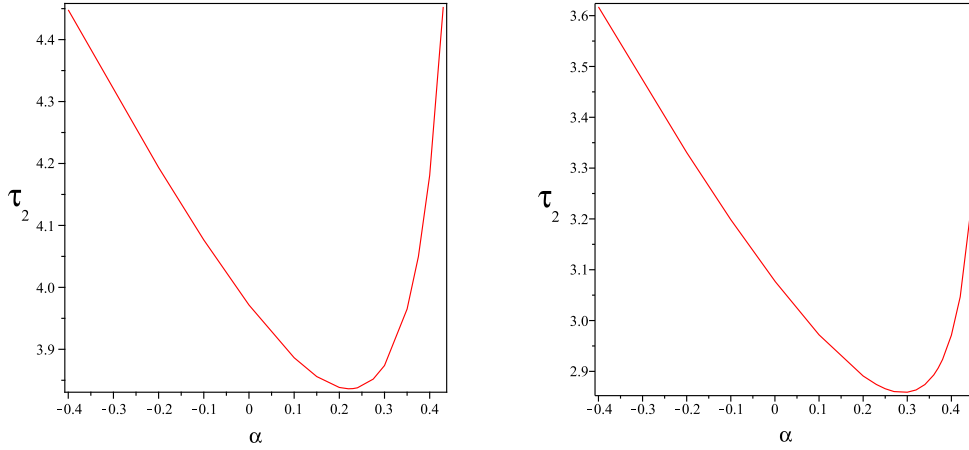


Figure 1: τ_2 vs α in 5-dimensions with $z = 2$. Left: neutral black holes with $\alpha_m \approx 0.22$. Right: weakly charged black holes ($\tilde{Q} \approx 0.676 \tilde{Q}_c$) with $\alpha_m \approx 0.3$. We have set $\ell = 1$.

with

$$\tau_z = \frac{r_0 f_0}{g_0}, \quad z \neq 1 \quad (4.2)$$

where f_0 and g_0 are (r_0, Q, α) -dependant coefficients from the near horizon expansions (3.18). Noting from eq. (2.12) that there is rescaling symmetry for $f(r)$, we write $f_0 \rightarrow \tilde{f}_0/\sqrt{r_0}$. Defining $\tilde{Q} \equiv Q/r_0^{n-1}$ we find numerically that τ_z is just a function of (\tilde{Q}, α) and does not depend on r_0 explicitly.

To examine the thermal behaviour of these charged Gauss-Bonnet black branes we follow two different approaches. First we investigate how temperature depends on the Gauss-Bonnet coefficient α for fixed electric charge. Then we investigate the variation of temperature with electric charge for fixed Gauss-Bonnet coefficient.

Consider first fixed electric charge \tilde{Q} . For $z = 1$ the temperature function τ_1 depends linearly on α as

$$\tau_1 = n\left(1 - \frac{\alpha}{\ell^2}\right) - \frac{\tilde{Q}^2}{2(n-1)}, \quad (4.3)$$

while numerical analysis indicates that the situation is different for $z > 1$. The reality condition from eq. (3.19) imposes the constraint $\alpha \leq \alpha_{\text{ext}}$, where

$$\alpha_{\text{ext}} = \frac{2n^2 + 2(z-2)n + 2(z-1)^2 - \tilde{Q}^2}{2n^2 + 2(2z-3)n + 4(z-1)^2} \ell^2. \quad (4.4)$$

Recalling that $\alpha < \ell^2/2$, we define $\tilde{Q}_c = \tilde{Q}(\alpha_{\text{ext}} = \ell^2/2)$ from (4.4), yielding

$$\tilde{Q}_c^2 \equiv n(n-1). \quad (4.5)$$

For charged black holes with $\tilde{Q} < \tilde{Q}_c$ we have $\alpha_{\text{ext}} > \ell^2/2$ implying the bound $\alpha \leq \ell^2/2$; otherwise, if $\tilde{Q}_c < \tilde{Q} < \tilde{Q}_{\text{ext}} (= Q_{\text{ext}}/r_0^{n-1})$ then $\alpha < \alpha_{\text{ext}} < \ell^2/2$.

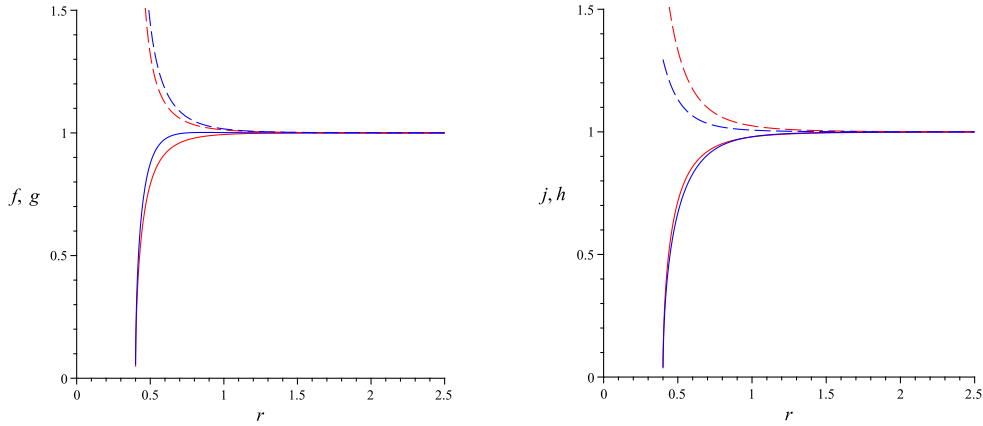


Figure 2: Functions describing 5-dimensional neutral Einstein ($\tilde{Q} = 0, \alpha = 0$) in red lines and neutral Gauss-Bonnet ($\tilde{Q} = 0, \alpha = 0.36$) in blue lines both with $z = 2$. Left: metric functions $f(r)$ (solid) and $g(r)$ (dashed). Right: gauge functions $j(r)$ (solid) and $h(r)$ (dashed). We have set $\ell = 1$.

Numerically solving the field equations, we find that weakly charged ($\tilde{Q} < \tilde{Q}_c$) or neutral black holes with $z > 1$ get colder as α decreases from its maximal value of $\ell^2/2$ down to a specific value, denoted α_m , which can be determined numerically. As α further decreases below α_m the temperature starts increasing. In other words the temperature is minimized at $\alpha = \alpha_m < \ell^2/2$.

We depict this behaviour in fig. 1 for small and large black holes in 5 dimensions with $z = 2$. It is evident from fig. 1 that it is possible to find isothermal pairs of black holes. For example, a $z = 2$ neutral Einstein black hole ($\alpha = 0$) with $r_0 = 0.4$ is isothermal to a neutral GB black hole with $\alpha = 0.36$ of the same z and size. We illustrate in fig. 2 that these are indeed two different solutions.

For charged black holes with intermediate values of the electric charge – $\tilde{Q} \lesssim \tilde{Q}_c$ – we find that the temperature has a minimum nonzero value at $\alpha \lesssim \ell^2/2$ and then increases monotonically as α decreases from $\ell^2/2$. There are no isothermal pairs. We illustrate this behaviour for typical cases in the left-hand side of fig. 3.

The temperature T of strongly charged GB black holes, where $\tilde{Q} > \tilde{Q}_c$ (and $z > 1$) exhibits markedly different behaviour. In this case $\alpha < \alpha_{\text{ext}} < \ell^2/2$ and we find, as shown in the right-hand side of fig. 3, that T starts from zero at $\alpha = \alpha_{\text{ext}}$ and then monotonically increases with decreasing α . Again, no isothermal pairs occur.

Turning next to the question of how temperature changes with charge for fixed α , we shall consider separately the high temperature and low temperature behaviour.

For a given α , high temperature behaviour corresponds to $\tilde{Q} \rightarrow 0$. In this limit the temperature function τ_z is just a function of α and independent of r_0 . Hence $T \propto r_0^z$ for charged GB black holes at high temperature with arbitrary z .

We have already noted that in the high temperature limit there exist pairs of isothermal black holes with different GB coefficients, one with $\alpha > \alpha_m$ and the other

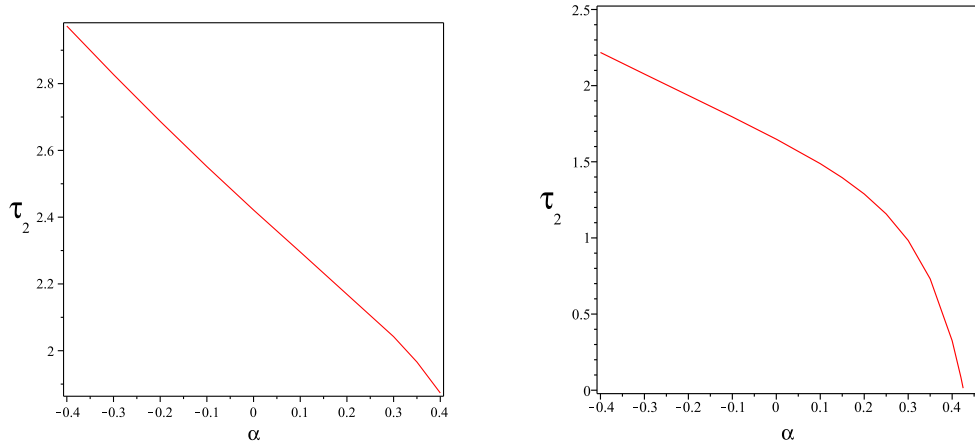


Figure 3: τ_2 vs α in 5-dimensions with $z = 2$. Left: intermediate charged black holes ($\tilde{Q} \approx 0.902 \tilde{Q}_c$) with $\alpha_{\text{ext}} \approx 0.55$. Right: strongly charged black holes ($\tilde{Q} \approx 1.128 \tilde{Q}_c$) with $\alpha_{\text{ext}} \approx 0.425$. We have set $\ell = 1$.

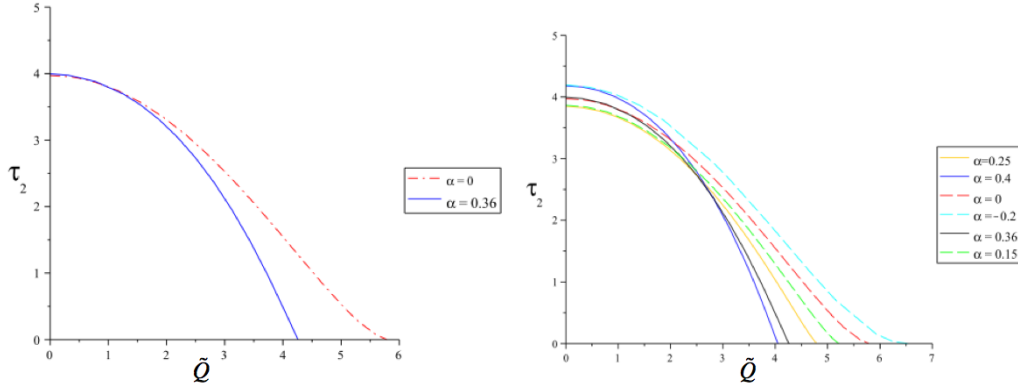


Figure 4: τ_2 vs \tilde{Q} for $z = 2$ black holes in 5 dimensions with $\alpha_m \approx 0.22$. In the right hand plot solids show $\alpha > \alpha_m$ where dashed show $\alpha < \alpha_m$.

with $\alpha < \alpha_m$. (The minimum GB coefficient $\alpha_m \approx 0.22$, 0.02 and -0.1 for $z = 2$, 3 and 4 respectively). We consider two such isothermal cases in fig. 4. We see that for small \tilde{Q} (or high temperature) the plots for the isothermal pairs $\alpha = (0, 0.36)$ and $\alpha = (-0.2, 0.4)$ (where $\alpha_m \simeq 0.22$) are essentially the same.

However the distinction between pairs grows with increasing \tilde{Q} . As the low temperature limit ($\tilde{Q} \rightarrow \tilde{Q}_{\text{ext}}$) is approached, the behaviour of τ_z becomes significantly different between the elements of the isothermal pair. For $\alpha < \alpha_m$ the low temperature limit ($T \rightarrow 0$) is non-linear as a function of increasing \tilde{Q} , whereas for its isothermal counterpart with $\alpha > \alpha_m$, it tends toward linearity. We will revisit this distinction in the next section where we will discuss the behaviour of the specific heat at low temperature.

Fig. 4 illustrates this for $z = 2$. The same situation occurs for arbitrary values of $z > 1$, as shown in fig. 5 for $z = 3$. We conclude that this is a general feature of

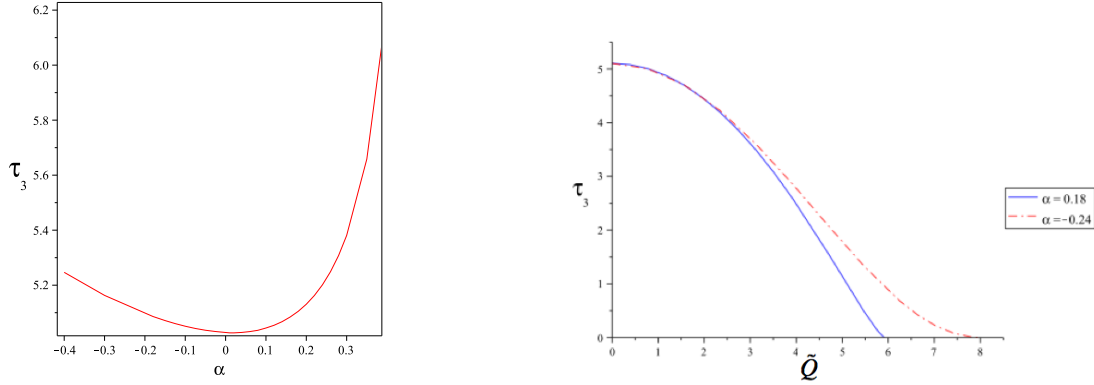


Figure 5: Left: τ_3 vs α for 5-dimensional $z = 3$ neutral black holes. Right: τ_3 vs \tilde{Q} for 5-dimensional $z = 3$ GB black holes with $\alpha = 0.18$ (blue) and $\alpha = -0.24$ (red) [$\alpha_m \approx 0.02$].

planar Gauss-Bonnet black holes of arbitrary size and $z > 1$.

In general for a given z , black holes with $\alpha < \alpha_m$ show non-linear behaviour at low temperature. As α decreases below α_m , the maximum temperature, $T(Q = 0)$, increases as does Q_{ext} . As a result the non-linearity at low temperature becomes more significant as α/α_m becomes smaller. However as α increases above α_m , the maximum black hole temperature increases while Q_{ext} decreases. In other words the temperature falls faster, with the low temperature behaviour becoming increasingly linear as shown in fig. (4-right).

We close this section by noting that for $\alpha = \alpha_m$ no isothermal pairs exist.

4.2 Specific heat and Fermi liquid behaviour

The specific heat at fixed volume is given by:

$$C = T \frac{(dS/dr_0)}{(dT/dr_0)} \quad (4.6)$$

where

$$S = \frac{1}{2} \frac{\pi^{n/2} r_0^{n-1}}{\Gamma(\frac{n}{2})} \quad (4.7)$$

is the Bekenstein-Hawking entropy of the black brane. A characteristic behaviour of a Fermi liquid is that its specific heat depends linearly on temperature. A recent study of Fermi liquid holography compared asymptotically AdS charged Einstein black holes ($z = 1$) to asymptotically Lifshitz ones ($z > 1$) [23]. The former obeyed Fermi liquid behaviour at low temperature, whereas the latter did not. Instead asymptotically Lifshitz Einstein-Maxwell black holes ($z > 1$) at low temperature deviate from Fermi liquid behaviour. Indeed, for this class of black holes C/T diverges in the $T \rightarrow 0$ limit.

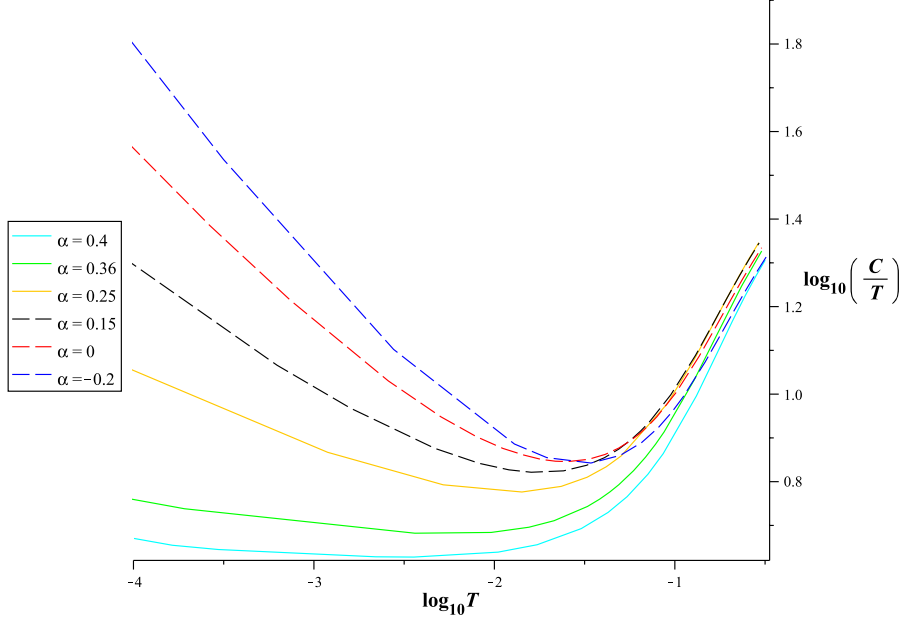


Figure 6: $\log_{10}(C/T)$ vs $\log_{10} T$ in 5 dimensions with fixed charge $Q = 1$, $z = 2$, and $\alpha_m \approx 0.22$.

To see how the GB correction modifies specific heat, we begin with the $z = 1$ case. Here we can easily obtain an analytic expression for the specific heat

$$\frac{C}{T} = \frac{4(n-1)^2 \pi^{\frac{n}{2}+1} r_0^{n-2}}{\Gamma(\frac{n}{2}) \left[(2n-3)\tilde{Q}^2 + 2n(n-1)(1 - \frac{\alpha}{\ell^2}) \right]} \quad (4.8)$$

using eqs. (4.1), (4.3) and (4.7). From eq. (4.8) it is straightforward to show that at high temperature (i.e. $\tilde{Q} \rightarrow 0$) the Sommerfeld ratio $C/T \propto T^{n-2}$. However at low temperature, where the electric charge approaches the extremal value $\tilde{Q}_{\text{ext}} (= Q_{\text{ext}}/r_0^{n-1})$ introduced in (3.20), the Sommerfeld ratio becomes constant:

$$\frac{C}{T} \rightarrow \frac{\pi^{\frac{n}{2}+1} r_{\text{ext}}^{n-2}}{n\Gamma(\frac{n}{2})(1 - \frac{\alpha}{\ell^2})} \quad \text{as} \quad T \rightarrow 0 \quad (4.9)$$

with

$$r_{\text{ext}} = \left[\frac{Q^2}{2n(n-1)(1 - \frac{\alpha}{\ell^2})} \right]^{\frac{1}{2n-2}} \quad (4.10)$$

The low-temperature constancy of the Sommerfeld ratio is a key characteristic of Fermi liquids.

We have already observed that $T \propto r_0^z$ for arbitrary values of z in the high temperature ($\tilde{Q} \rightarrow 0$) limit. Consequently, since specific heat is proportional to r_0^{n-1} , we find that $C \propto T^{(n-1)/z}$ for all GB black holes.

The low temperature limit C/T for $z > 1$ must be obtained numerically. We have numerically computed the specific heat (4.6) for a range of values of α . In fig.

6 we plot the Sommerfeld ratio C/T as a function of temperature on a log-log scale for $z = 2$ for the isothermal pairs in fig. 4. We see although both $\alpha < \alpha_m$ and $\alpha > \alpha_m$ are isotherm pairs at high temperature, dramatic growth appears in C/T as $T \rightarrow 0$ for $\alpha < \alpha_m$, increasingly so as α becomes much smaller than α_m . Therefore the low temperature behaviour becomes increasingly non-linear for GB black holes with $\alpha < \alpha_m$, with the Sommerfeld ratio depending on temperature as a weak power law, consistent with the prediction of the Castro Neto et al. model. The slope of the line in the log-log plot of C_V/T at low temperature from the bulk depends on the value of α , whereas for the Castro Neto et al. model it is characterized by $\lambda - 1$. For example, for $\alpha = -0.2$ the slope is approximately -0.43 (corresponding to $\lambda = 0.57$) while it is approximately -0.38 for $\alpha = 0$ (equivalent to $\lambda = 0.62$).

The $\alpha > \alpha_m$ isotherm counterparts exhibit rather different behaviour at low temperature, with the T -dependence of the Sommerfeld ratio showing vanishingly small power law behaviour as α increases (corresponding to $\lambda \rightarrow 1$). For $\alpha \gg \alpha_m$, this becomes almost constant, restoring Fermi liquid behaviour.

5. Closing remarks

Adding a Gauss-Bonnet term to the Einstein-Hilbert action results in interesting low temperature behaviour for asymptotically Lifshitz charged black holes. By investigating the thermodynamic properties of such black holes at low temperature, we found that the Sommerfeld ratio γ_0 is temperature dependent, governed by a weak power law behaviour depending on the value of α . This kind of behaviour is a characteristic property of some heavy fermion metals such as f-electron compounds at low temperature. A CM model of these non-Fermi liquids [9, 10] predicts weak power law behaviour for other properties such as heat capacity and susceptibility, i.e. $\gamma_0(T) \equiv C(T)/T \propto \chi(T) \propto T^{-1+\lambda}$ with $\lambda < 1$.

We propose that Lifshitz-GB charged black holes are gravitational duals to the Castro Neto et al. model [9, 10], with the Gauss-Bonnet coefficient α holographically dual to the characteristic parameter λ . To more firmly establish this duality will involve a study of other thermodynamic quantities like resistivity or susceptibility using the gravity theory. We leave this topic for future work.

Acknowledgements

This work was supported by the Natural Sciences and Engineering Research Council of Canada.

References

- [1] J. M. Maldacena, *The large N limit of superconformal field theories and supergravity* Adv. Theor. Math. Phys. **2**, 231 (1998)[Int. J. Theor. Phys. **38**, 1113 (1999)].
- [2] S. A. Hartnoll, *Lectures on holographic methods for condensed matter physics* JHEP [e-Print: arXiv:0903.3246].
- [3] D. S. Rokhsar and S. A. Kivelson, *Superconductivity and the Quantum Hard-Core Dimer Gas* Phys. Rev. Lett. **61** 2376 (1988).
- [4] E. Ardonne, P. Fendley and E. Frandkin, *Topological order and conformal quantum critical points* Annal Phys. **310** 493 (2004).
- [5] A. Vishwanath, L. Balents, and T. Senthil, *Quantum Criticality and Deconfinement in Phase Transitions Between Valence Bond Solids* Phys. Rev. B **69** 224416 (2004).
- [6] G. R. Stewart, Heavy-fermion systems, Rev. Mod. Phys. **56**, 755 (1984); G. R. Stewart, Non-Fermi-liquid behavior in d- and f-electron metals, Rev. Mod. Phys. **73**, 797 (2001) [Addendum-ibid. **78**, 743 (2006)]. [4] H. v. Lohneysen, A. Rosch, M. Vojta and P. Wölfle, Fermi-liquid instabilities at magnetic quantum phase transitions, Rev. Mod. Phys. **79**, 1015 (2007).
- [7] H.v. Lohneysen, T. Pietrus, G. Portisch, H.G. Schlager, A. Schroder, M. Sieck, and T. Trappmann, Non-Fermi Liquid Behavior in a Heavy-Fermion Alloy at a Magnetic Instability, Physical Review Letters **72** 3262 (1994).
- [8] *Conference on Non-Fermi liquid behavior in Metals*, J. Phys. Cond. Mat **8**, 1996.
- [9] A. H. Castro Neto, G. Castilla and B. A. Jones, Phys. Rev. Lett. **81**, 3531 (1998).
- [10] A. H. Castro Neto and B. A. Jones, Phys. Rev. **B62**, 14975 (2000).
- [11] M. C. de Andrade, R. Chau, R. P. Dickey, N. R. Dilley, E. J. Freeman, D. A. Gajewski, M. B. Maple, R. Movshovich, A. H. Castro Neto, G. E. Castilla and B. A. Jones, *Evidence for a common physical description of non-Fermi-liquid behavior in f-electron systems*, Phys. Rev. Lett. **81**, 5620 (1998).
- [12] R. Vollmer, T. Pietrus, H. v. Löhneysen, R. Chau, and M. B. Maple, *Phase transitions and non-Fermi-liquid behavior in UCu_5Pd_x at low temperatures*, Phys. Rev. **B61**, 1218 (2000).
- [13] P. Coleman and A.J. Schofield, Quantum criticality, Nature **433** (2005) 226 [arXiv:cond-mat/0503002].
- [14] S. Kachru, X. Liu and M. Mulligan, *Gravity Duals of Lifshitz-like Fixed Points* Phys. Rev. D **78** 106005 (2008).

- [15] E. J. Brynjolfsson, U. H. Danielsson, L. Thorlacius and T. Zingg *Black Hole Thermodynamics and Heavy Fermion Metals* JHEP **1008** 027 (2010) [e-Print: arXiv:1003.5361].
- [16] R. Gregory, S. Kanno, and J. Soda, “Holographic Superconductors with Higher Curvature Corrections” JHEP **0910** 010 (2009).
- [17] Q.Y. Pan, B. Wang, E. Papantonopoulos, J. Oliveria, and A.B. Pavan, “Holographic Superconductors with various condensates in Einstein-Gauss-Bonnet gravity ” Phys. Rev. **D81** 106007 (2010) arXiv:0912.2475 [hep-th].
- [18] X.H. Ge, B. Wang, S.F. Wu, and G.H. Yang, “Analytical study on holographic superconductors in external magnetic field” arXiv:1002.4901 [hep-th].
- [19] Q.Y. Pan and B. Wang, “General holographic superconductor models with Gauss-Bonnet corrections” arXiv:1005.4743 [hep-th].
- [20] U. H. Danielsson and L. Thorlacius *Black holes in asymptotically lifshitz spacetime* JHEP **0903** 070 (2009).
- [21] R. B. Mann *Lifshitz Topological Black Holes*, JHEP **0906** 075 (2009).
- [22] G. Bertoldi, B. A. Burrington and A. Peet, *Black holes in asymptotically Lifshitz spacetimes with arbitrary critical exponent*, Phys. Rev. **D80** 126003 (2009) [arXiv:0905.3183].
- [23] E. J. Brynjolfsson, U. H. Danielsson, L. Thorlacius and T. Zingg *Holographic models with anisotropic scaling* [e-Print: arXiv:1004.5566]
- [24] M. H. Dehghani, R. B. Mann and R. Pourhasan *Charged Lifshitz Black Holes* [e-Print: arXiv:1102.0578]
- [25] M. H. Dehghani, R. B. Mann *Lovelock-Lifshitz Black Holes* JHEP **07** 019 (2010) [e-Print: arXiv:1004.4397]
- [26] M. H. Dehghani, R. B. Mann *Thermodynamics of Lovelock-Lifshitz Black Branes* Phys. REv. **D82** 064019 (2010) [e-Print: arXiv:1006.3510]
- [27] G. Bertoldi, B. A. Burrington and A. W. Peet, *Thermodynamics of black branes in asymptotically Lifshitz spacetimes* Phys. Rev. **D80** 126004 (2009) [arXiv:0907.4755]
- [28] D. Pang *On Charged Lifshitz Black Holes* [e-Print: arXiv:0911.2777]